

# New Approach to Establish a Clear Sky Global Solar Irradiance Model

Mohamed ZAIANI \*, Djelloul DJAFER \*, Fatima CHOUIREB \*\*

\*Unité de Recherche Appliquée en Energies Renouvelables, URAER, Centre de Développement des Energies Renouvelables, CDER, 47133, Ghardaia, Algeria

\*\*Laboratoire des Télécommunications, Signaux et Systèmes LTSS, Université Amar Telidji de Laghouat, Algeria

mohamed\_zaiani@hotmail.fr, djджаfer@gmail.com, chouirebfatima@yahoo.com

Corresponding author: first Author, mohamed\_zaiani@hotmail.fr

*Received: 01.03.2017 Accepted: 14.02.2017*

**Abstract-** Prediction of Global Solar Radiation of a given location is useful to obtain the correct design of solar equipments in the case of a clear sky conditions. We have developed a new approach to establish a GSR model using 10 years of measurements. This model allows the prediction of GSR to any a given clear day of the year. Results show that our model predicts the daily GSR with  $R^2$  of 0.982 and MBE of 7.937. In addition a good correlation between daily average values of the measured and predicted GSR is found (0.940 for  $R^2$ , 2.711 % for MAPE, 20.9 for RMSE and 2.727 for MBE).

**Keywords** Solar radiation, GSR prediction, Neural Network, MultiLayer Perceptron method

## 1. Introduction

Solar radiation is the direct form of abundant permanent solar energy resource available on earth, due to nuclear fusion on Sun. Earth surface is receiving about one hundred thousand TW of this renewable energy of solar power at earth's surface at each moment. Unfortunately, the Solar Radiation measurements are not easily available because of the cost of measuring equipments and the maintenance and calibration requirements. Therefore, it is rather important to elaborate methods to estimate the solar radiation to use it for solar energy applications including the design and analysis of energy-conversion devices and architectural design. However, the solar radiation has three components which are: Global Solar Radiation (GSR), Direct Solar Radiation and Diffuse Solar Radiation.

The value of the Global Solar Radiation (GSR) is the most important parameter for solar energy applications [1, 2, 23]. Studying the behavior of solar radiation to a given location requires long-term data and require the use empirical, semi-empirical, physical, neural networks techniques [4, 5]. Many studies are performed by researchers to estimate or predict

solar radiation using available meteorological and geographical parameters such as sunshine hours, air temperature, relative humidity and latitude [6, 7, 8, 9,10, 11].

The most common parameter to simulate GSR is sunshine duration [10, 12, 13], mainly due to the fact that sunshine duration can be easily and reliably measured. All models, which are presented in the literature, have used different SRTs (Statistical Regression Techniques) to find empirical coefficients of models [10, 12, 14] and other techniques [5, 15, 16] in order to estimate or predict solar radiation based on daily values. Most of authors were interested by the prediction of the hourly or daily mean values [18, 19, 2, 4, 17, 20] and not for instantaneous daily GSR. Nevertheless, in the present work, we will establish a model that estimates and predicts the GSR for any time of a given day of the year. This model is based on four important inputs which are: the Full Width at Half Maximum (FWHM) of the clear day GSR component, its maximum value, the Angstrom coefficient and the Angstrom exponent. The Artificial Neural Network (ANN) based on MultiLayer Perceptron (MLP) will be used to calculate the different parameters of this model. After a brief introduction in section 1, the section 2 provides the site characterization

and data used. In section 3 we discuss the proposed approach and which parameters will be used to characterize the ANN

**Table1.** Number of clear days (N) per year.

year	2004	2005	2006	2007	2008	2009	2010	2011	2012	2013
N	54	93	93	117	68	68	45	48	86	50

model, section 4 presents the methodology to establish the neural network model and in section 5 we discuss the obtained results comparing with Perrin model.

## 2. Site and Used Data Base

This work is performed using 10 years of data (from August 2004 to December 2013) collected at the the Unit of Applied Research in Renewable Energy (Ghardaia, Algeria). The detail of the instruments and methods of the data collection are described by Djafer and Irbah [21]. The key to know is that the three components of solar radiation (global, diffuse and direct) are recorded every 5 minutes since 2004 in addition to temperature and humidity. The instruments that measure the direct, the global and the diffuse solar radiation components are of EKO type, which are usually cleaned two or three times per week according to the weather conditions (Fig.1). They are also regularly calibrated at the meteorological station of Tamanrasset (latitude = +22.78°, longitude = +5.51°, altitude = 1270 m) where the solar irradiance is measured since 1970.

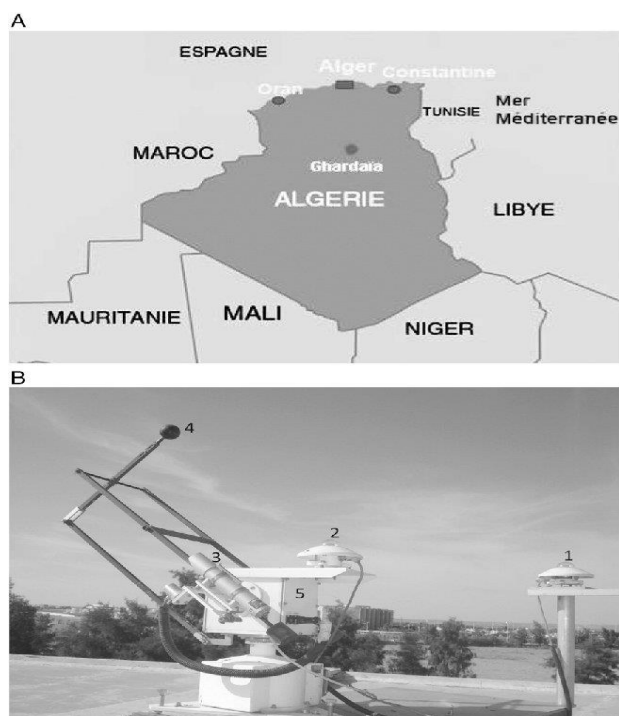


**Fig. 1.** Location of Ghardaia city (top). Instrumentation station (bottom) for measuring the global, the direct and the diffuse solar radiation: (1)Pyranometer for measuring the global solar irradiance. (2) Pyranometer for measuring the diffuse

irradiance component. (3) Peryheliometer for measuring the direct irradiance component. (4) The ball used to permanently hide the pyranometer (2). (5) The 2-axis solar tracker.

## 3. Description of the Proposed Approach

In our approach, the GSR is modeled by using a polynomial of fourth degree with coefficients  $a_j$  ( $j=0..4$ ), these coefficients are the outputs of the ANN created model of the clear day. The inputs of the ANN model are M, FWHM,  $\alpha$  and  $\beta$ . The way to establish the model is described in the following paragraphs.

We will select the totality of clear days determined by the wavelet method described by Djafer and al [11]. Table 1 summarizes the number of clear days (N) per year and Fig.2 shows a GSR of two clear days.

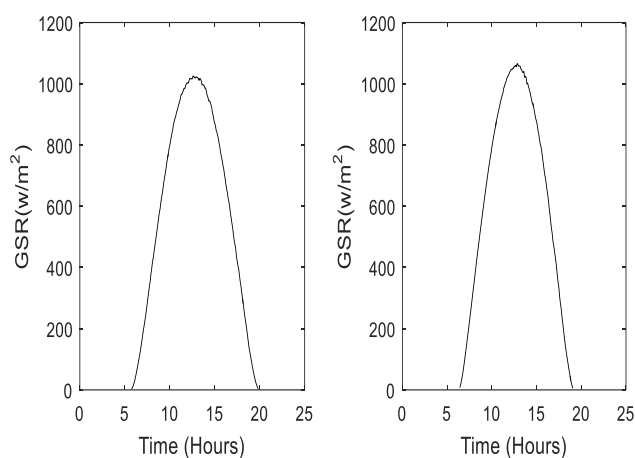


**Fig. 2.** Global Solar Radiation components for two clear days (26/6/2004 and 11/4/2005).

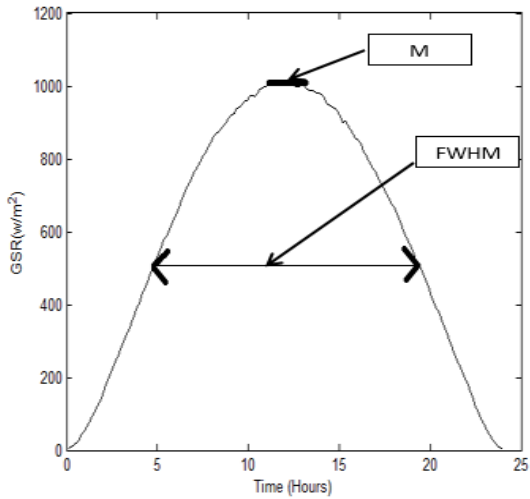


**Fig. 3.** Determination of the maximum  $M$  of a clear day GSR and its FWHM.

For each clear day, we determine the maximum ( $M$ ) of the GSR and its FWHM as shown in Fig.3. Figure 4a and 4b illustrate respectively the daily variation of  $M$  and FWHM of the year 2005. Figure 5a and 5b represent the temporal variation of these two parameters from 2004 to 2013. The daily average variation of these two parameters as function of time and declination are shown respectively in Fig.6 and Fig.7.

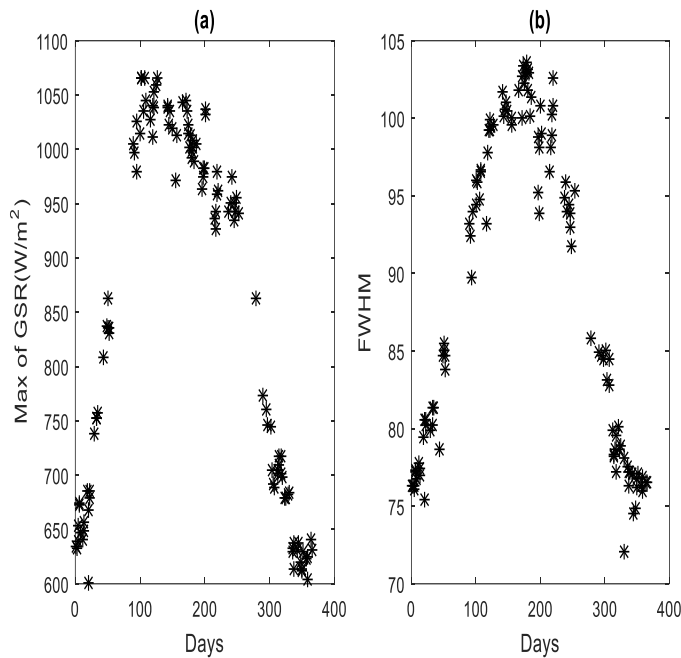


**Fig. 4.** (a) Daily variation of the maximum  $M$  of clear days GSR during 2005, (b) daily variation of the FWHM of clear days GSR during 2005.

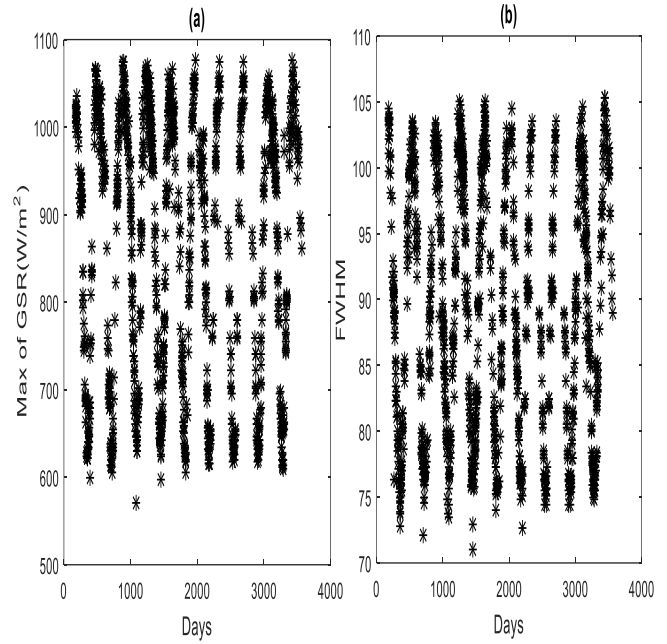


**Fig. 5.** (a) Temporal variation of the maximum values ( $M$ ) of clear days GSR between 2004 and 2013, (b) temporal variation of FWHM of clear days GSR between 2004 and 2013.

According to Fig.6b, the daily average variation of the parameter FWHM is a regular Gaussian which is not the case for the daily average variation of the maximum  $M$  that shows a Gaussian shape with a linear regression between May and October. This behavior is confirmed by Fig.7b where we find a linear regression of FWHM with declination and not quite linear with the maximum  $M$ .

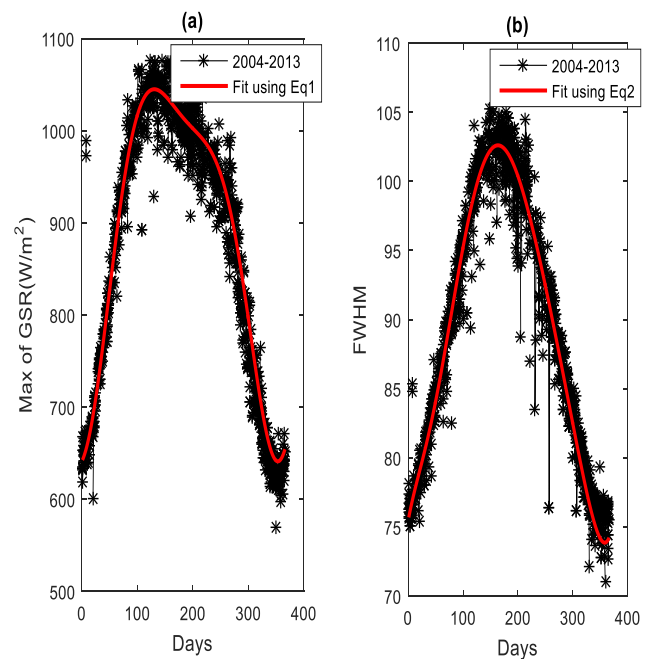


**Fig. 6.** (a) Daily average variation of  $M$  between 2004 to 2013. (b) daily average variation of FWHM between 2004 to 2013.

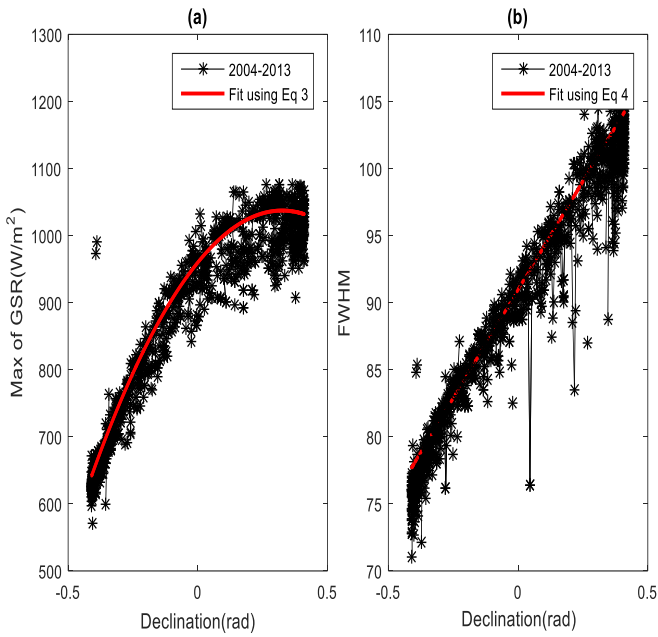


**Fig. 7.** (a) Daily average variation of M as a function of Declination (rad). The variation of these two parameters with time are modeled each by a polynomial of degree 8 (equation 1 and equation 3) and their variation with declination by linear regression for FWHM (equation 4) and polynomial second degree for M (equation 2). The analytical expressions of these equations are as follow:

$$M(d) = a_0 + a_1.d + \dots + a_8.d^8 \tag{1}$$

$$M(\theta) = a_0 + a_1.\theta + a_2.\theta^2 \tag{2}$$

$$FWHM(d) = b_0 + b_1.d + \dots + b_8.d^8 \tag{3}$$

$$FWHM(\theta) = b_0 + b_1.\theta \tag{4}$$

Where  $d$  is the day number of the year and  $\theta$  is the declination. We will compare which of these equations will be used hereafter, either the M and FWHM as function of  $d$  or as function of  $\theta$ . The statistical analysis between the two possibilities using all the clear days of Table 1 are given in Table 2. We note that the equations (1) and (3) give the best results. Therefore, they will be used hereafter to perform the present study.

The first step to implement our model is that: for each clear day GSR we fit it with an analytical function. The adopted function to perform the fit is given by the following equation:

$$GSR(t) = a_0 + a_1.t + a_2.t^2 + a_3.t^3 + a_4.t^4 \tag{5}$$

declination between 2004 to 2013, (b) daily average variation of FWHM as a function of declination between 2004 to 2013.

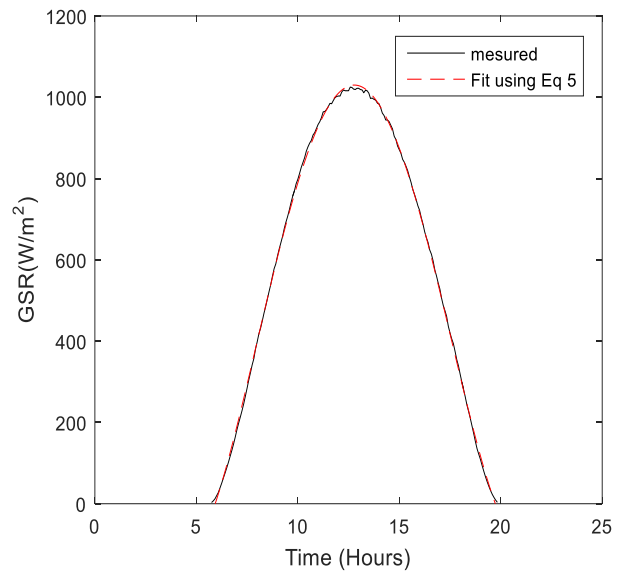


**Fig. 8.** The measured clear day GSR (black line) at 26/6/2004 superposed to modeled one (dashed line).

Equation (5) is a polynomial of fourth degree with coefficients  $a_j$  ( $j=0-4$ ) and  $t$  is the time of collection with a step of 5 minutes. Figure 8 represents a clear day GSR (black line) superposed to the modeled one (red dashed line). Therefore, for each clear day GSR we will have a vector  $x$  of six coefficients ( $a_0, a_1, a_2, a_3, a_4, d$ ) that correspond to a defined day  $d$  in the year. We repeat the same process for  $N$  clear days of Table 1. At the end we will have a matrix of dimension  $N \times A$ , with  $A$  equal 6, the length of the vector  $x$ . Each row of this matrix represents a GSR for a given day  $d$ . Since, it is impossible to have all days of a year as clear days, we should build a model that permits to have the GSR for any given day of the year. To do that, we will use the matrix data

described above to develop a model using a Neural network based on MultiLayer Perceptron (MLP) algorithm. The way to find the optimum ANN model is developed in the next section.

#### 4. Validation of the ANN Model

A formal neuron is a nonlinear algebraic function bounded whose value depends on the settings called weights. The values of this function are the inputs of the neuron and the obtained values from this function are outputs. Figure 9 shows a formal neuron model representation [23].

The neural network method used in our present work is based on MultiLayer Perceptron (MLP), the most common type used of neural networks. MLP consists of the input layer, output layer, and one or more hidden layers [19].

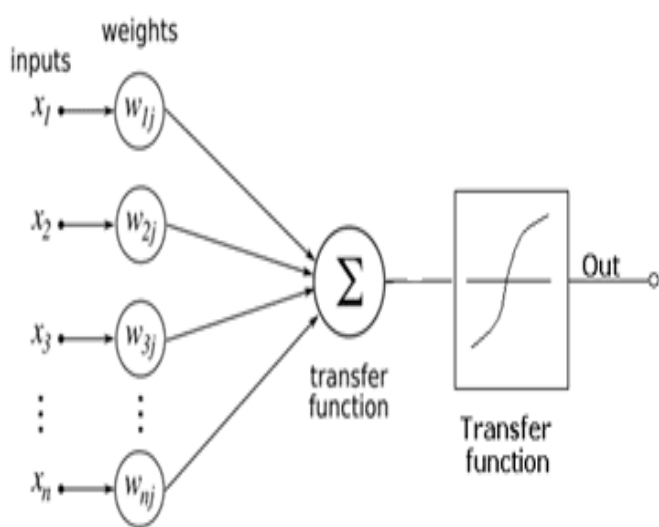


Fig. 9. Formal Neural Network.

Each layer of MLP includes one or more neurons directionally linked with the neurons from the previous and the next layer. For instance, Fig.10 represents a 3-layer perceptron with three inputs, two outputs, and a hidden layer of five neurons. To determine the appropriate network architecture of MLP to be used to estimate or predict the coefficients of Equation (5), we have tried several numbers of neurons in the hidden layer, several learning functions and several numbers of inputs.

In our case, the inputs of the model are the values of the maximum  $M$  of clear days GSR and its FWHM in addition to two turbidity parameters, the Angstrom exponent  $\alpha$  and the

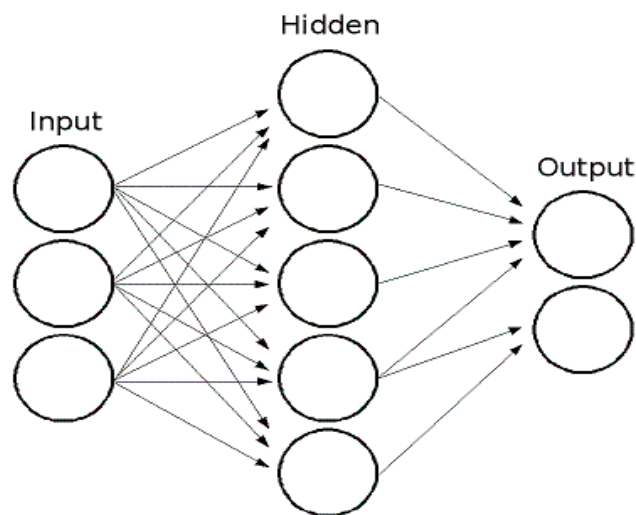


Fig. 10. A three layers Multilayer Perceptron architecture.

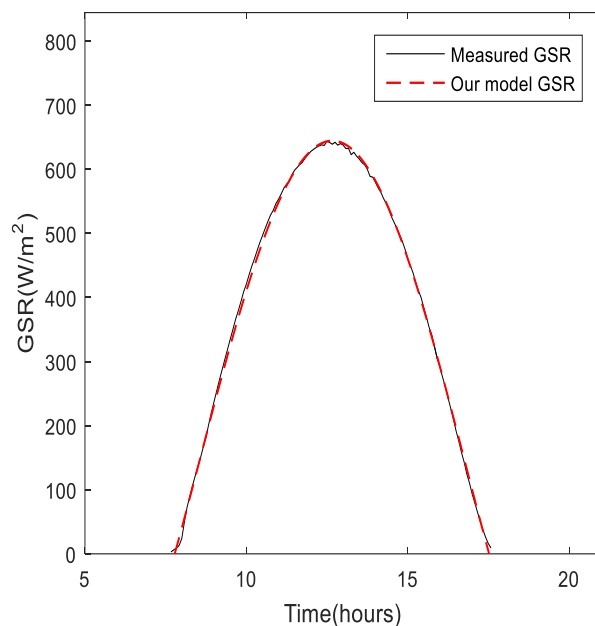


Fig. 11. The measured GSR (black line) in 09/12/2007 superposed to the calculated

Angstrom coefficient  $\beta$  calculated from MODIS data [24]. For the outputs of the MLP, they are the coefficients of Equation (5). Our model will be compared to the Perrin model described in [25, 26, 27], which have been widely used for estimating solar radiation for the same area [28, 29]. The direct Solar radiation ( $I$ ), the Diffuse Solar Radiation ( $D$ ) and the Global Solar Radiation (GSR) are explained by the following equations [27, 26] :

$$I = I_0 * \sin(h) \tag{6}$$

$$D = 125 * (\sin(h))^{0.4} \tag{7}$$

$$GSR = I + D \tag{8}$$

According to Table 1, the total number of clear days during the ten years is 722 days. We have used 350 clear days in the learning and validating the ANN model. The remaining days will be used to perform the testing process.

The analysis of the accuracy of the obtained results and the performance of the ANN model is done by the calculation of the Mean Absolute Percentage Error (MAPE), Absolute Fraction of Variance ( $R^2$ ), the Root-Mean-Square Error (RMSE) and the Mean Bias Error (MBE). Closeness of MAPE to zero leads to high modeling accuracy. The Absolute Fraction of Variance expresses the correlation coefficient squared between two types of data. Likewise, the closeness of this amount to one, leads to a better modeling performance. The RMSE is used to figure out the degree of dispersion of the predicted GSR against the measured one, while the MBE is used to figure out the overestimation or underestimation of the predicted GSR, it gives an idea of the divergence between the estimated values and the measured values. A positive value shows over estimation and a negative value is under estimation. Equations used for calculating these statistical parameters are given below.

$$MAPE = \frac{1}{n} \sum_{i=1}^n \left| \frac{G_p - G_a}{G_a} \right| \times 100 \tag{9}$$

$$R^2 = 1 - \frac{\sum_{i=1}^n (G_p - G_a)^2}{\sum_{i=1}^n (G_a - \bar{G}_a)^2} \tag{10}$$

$$RMSE = \sqrt{\frac{1}{n} \sum_{i=1}^n (G_p - G_a)^2} \tag{11}$$

$$MBE = \frac{1}{n} \sum_{i=1}^n (G_p - G_a) \tag{12}$$

Where  $G_p$  is the daily predicted GSR and  $G_a$  the measured daily GSR on a horizontal surface.  $\bar{G}_a$  is the daily average of GSR during the period of measurements and  $n$  the number of observations. We should note that the statistical

**Table 3.** The accuracy of the ANN model in different situations.

Input parameters	ANN function	MAPE	$R^2$	RMSE	MBE
M and FWHM	Tansig-Tansig-Purelin	53.254	0.512	128.356	80.698
M and FWHM	Tansig-Purelin-Purelin	13.663	0.681	80.009	17.685
M and FWHM	Purelin-Purelin -Purelin	1.125	0.990	22.008	1.082
M, FWHM, $\alpha$ and $\beta$	Tansig-Tansig-Purelin	34.255	0.785	86.547	66.358
M, FWHM, $\alpha$ and $\beta$	Tansig-Purelin-Purelin	13.701	0.989	74.224	16.982
M, FWHM, $\alpha$ and $\beta$	Purelin-Purelin -Purelin	0.930	0.995	5.939	0.661

errors are calculated between the daily measured and predicted GSR which are collected every 5 min. Therefore the daily averages are obtained for all clear days per year.

To test this empirical ANN model we use the remaining values of M and FWHM (372 clear days GSR as stated above). these values are feed to the ANN model to determine the coefficients of equation (5) and consequently the calculated GSR. Figure 12a shows an example of a measured GSR superposed to the calculated one. Figure 12b represents the measured daily average GSR as a function of the calculated one by our model in addition to the linear equation that governs the relation between them.

The fit quality of the calculated GSR to the measured one is evaluated by MAPE,  $R^2$ , RMSE and MBE. As it has been stated above, we perform the process by changing the types of functions of ANN and the number of inputs(see first and second column of table 3). The result of evaluation using tangent sigmoid transfer function and a linear transfer function (purelin) in the final layer is summarized in Table 3.

According to the values of  $R^2$ , MAPE, RMSE and MBE the Purelin–Purelin–Purelin configuration with four inputs parameters is the best one,  $R^2$ , MAPE, RMSE and MBE are 0.995, 0.930, 5.939 and 0.661 respectively. This configuration has been used to test the ANN model and it will be considered as our model with FWHM and M obtained by using Equation (1) and (3) as input of the ANN model.

In this stage we have used the M and FWHM of the 372 remaining days to evaluate our model. The results of this test are summarized by Fig.12. In Figure 12a we present a measured clear day GSR (black line) superposed to the calculated one by our model (red dashed line). We have compared the measured daily average GSR with that calculated by our model and Fig.12b shows the correlation between them. The difference between the measured and the calculated GSR by our model shows average values of 0.995 for  $R^2$ , 0.930 for MAPE, 5.939 for the Root Mean Square Error (RMSE) and 0.661 for MBE.

**5. Results and Discussion**

In this stage we will test our proposed model described by the diagram shown in Fig.13 using all the dates ( $d$ ) of clear days of Table 1. Firstly, for each given day  $d$ , we determine the  $M$  and  $FWHM$  using Equation (1) and (3). Then, the calculated values of  $M$  and  $FWHM$  in addition to the two turbidity parameters  $\alpha$  and  $\beta$ , are feed as inputs to our ANN model described in the above section to get the coefficients of equation (5) and to calculate the corresponding  $GSR(t)$ .

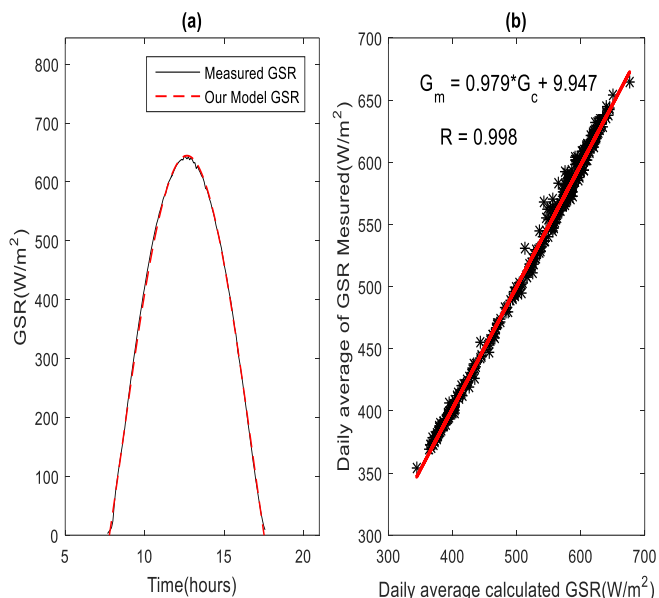


**Fig. 12.** (a) A measured GSR (black line) superposed to the calculated one (dash line)(day 25/11/2006), (b) daily average of both GSR model and measured.

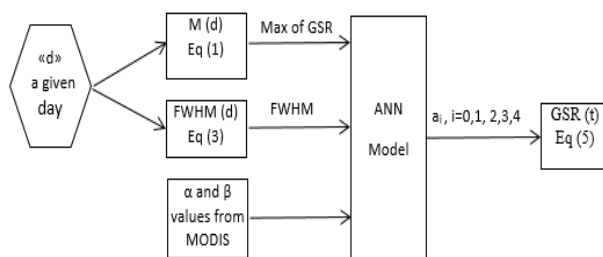


**Fig. 13.** Diagram of our developed model.

**Table 4.** Statistical analysis of the difference between the measured and the calculated GSR.

Statistical		2004	2005	2006	2007	2008	2009	2010	2011	2012	2013	Average
R <sup>2</sup>	Model	0.978	0.982	0.990	0.983	0.984	0.983	0.982	0.986	0.981	0.966	0.982
	Perrin	0.976	0.981	0.986	0.983	0.983	0.982	0.980	0.985	0.980	0.967	0.980
MAPE	Model	0.020	0.020	0.015	0.014	0.018	0.016	0.018	0.017	0.014	0.021	0.020
	Perrin	0.037	0.045	0.049	0.048	0.049	0.051	0.051	0.051	0.051	0.050	0.048
RMSE	Model	33.765	31.708	30.029	29.738	30.600	31.035	31.129	28.491	30.618	37.128	31.524
	Perrin	33.656	38.596	42.158	41.350	42.085	43.099	42.649	42.921	42.615	42.720	41.185
MBE	Model	7.937	7.635	-4.173	-0.403	8.044	2.172	8.058	5.558	3.241	-6.789	7.937
	Perrin	-5.549	-13.045	-19.611	-18.978	-21.116	-23.581	-23.396	-24.484	-23.901	-23.978	-19.764

Figure 14a represents a measured GSR(black line) superposed to the calculated GSR(red dashed line). The statistical analysis of the difference between the daily measured GSR and the calculated one for each year is given in Table 4. We note a good agreement between the measured and the calculated GSR. We have found that the yearly values of MAPE vary between 21.422 and 36.615, for R<sup>2</sup> between 0.966 and 0.990, for RMSE vary between 28.491 and 37.128, and those of MBE vary between -0.403 and 8.058. In addition, we have compared the daily average measured and calculated GSR(see Fig.14). The relation between them is approximated

by a straight line ( $G_m = G_c - 2.902$ ) where  $G_m$  is the average of the daily measured GSR and  $G_c$  is the average of the daily calculated GSR. This result shows good agreement between the daily average measured GSR and the calculated one. The found values of R<sup>2</sup>, the RMSE, MAPE and MBE are respectively 0.941, 20.90, 2.750 and 2.709.

We have compared our model to the Perrin model, we note that our model gives best results with an average of a correlation coefficient (R<sup>2</sup>) of 0.982, a root mean square error of 31.524 and MBE of 7.937 (see table 4 last column).

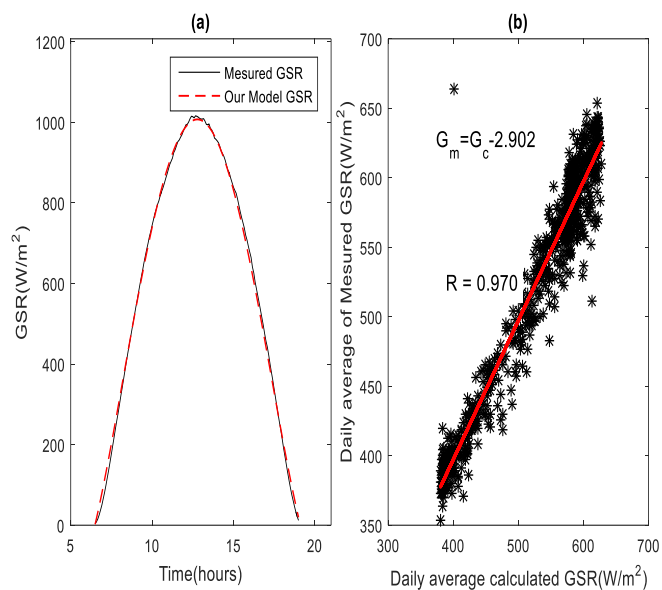


**Fig. 14.** (a) A measured GSR (black line) superposed to the calculated one (dashed line)(day 26/07/2004), (b) measured daily average GSR versus the calculated daily average GSR.

More detailed analysis was performed using the same methodology by using the hourly measured GSR. Table 5 represent the statistical errors between the measured GSR and our model GSR. The daily hourly average of RMSE varies between 27.125 and 35.964 and for the MBE varies between -0.009 and 0.670 for our model. We have compared the obtained results to the Perrin model. We note that our model gives best results with an average of RMSE equal to 30.277 and an average of MBE equal to 0.269.

**Table 5.** Statistical analysis of the difference between the hourly measured and the calculated GSR.

Statistical		2004	2005	2006	2007	2008	2009	2010	2011	2012	2013	Average
RMSE	Model	32.622	30.494	28.833	28.412	29.608	30.045	31.009	27.125	28.666	35.964	30.277
	Perrin	33.633	38.563	42.272	41.460	42.229	43.257	42.793	43.088	42.774	42.873	41.294
MBE	Model	0.614	0.622	-0.345	-0.009	0.670	0.172	0.650	0.497	0.314	-0.490	0.269
	Perrin	-0.493	-1.117	-1.655	-1.601	-1.777	-1.980	-1.963	-2.052	-2.004	-2.008	-1.665

## 6. Conclusion

In the present work we have proposed a new approach to establish a clear sky Global Solar Irradiance Model. This approach is composed of two steps. In the first one we calculate analytically the maximum values of GSR and its Full Width Half Maximum for any given day of the year in addition to the Angstrom coefficient ( $\beta$ ) and Angstrom exponent ( $\alpha$ ). These two turbidity parameters are determined from MODIS data. In the second, step these four parameters are fed to the chosen ANN model, the Purelin–Purelin–Purelin configuration that predicts the GSR with high precision ( $R^2 = 0.993$ , MAPE = 0.007). The output of this model is a polynomial coefficients that permit the calculation of GSR(t).

The analysis of the difference between the measured and the calculated GSR using 10 years of clear day measurements collected at the Unit of Applied Research in Renewable

Energy (Ghardaia, Algeria) show a good agreement between them. Results show that the yearly values of MAPE vary between 21.422 and 36.615, for  $R^2$  between 0.966 and 0.990, for RMSE vary between 28.491 and 37.128, and those of MBE vary between -0.403 and 8.058. The comparison between the daily average measured and calculated GSR has been performed.

We have found that the relation between them is approximated by a straight line with a correlation coefficient (R) of 0.970, a root mean square error of 20.90 and MBE of 2.727.

Also we have compared our model to the Perrin model where we have found that the proposed model gives best results. Finally our work presents a new approach to establish a model for clear sky conditions for a given location. Even though the proposed model can not be universally applied at the present time, since it is based on a measured data collected at the study area, but it might be generally used to predict the



GSR for regions with similar atmospheric and meteorological conditions as Ghardaia site. Furthermore, the advantage of the proposed approach can be used to have the GSR component in the case of problem of discontinuous to its measurement.

## References

- [1] V. Badescu, C. A. Gueymard, S. Cheval, C. Oprea, M. Baci, A. Dumitrescu, F. Iacobescu, I. Milos, and C. Rada. Accuracy analysis for fifty-four clear-sky solar radiation models using routine hourly global irradiance measurements in Romania. *Renewable Energy* 55, 85-103, 2013.
- [2] H. B. Tolabi, M. H. Moradi, and F. B. Tolabi. New Technique for Global Solar Radiation Forecast using Bees Algorithm. *International Journal of Engineering TRANSACTIONS B: Applications* Vol. 26, No. 11, 1385-1392, 2013.
- [3] M. J. Reno, C. W. Hansen, and J. S. Stein. Global Horizontal Irradiance Clear Sky Models: Implementation and Analysis. Sandia National Laboratories SAND2012-2389, 2012.
- [4] M. A. Mohandes. Modeling global solar radiation using Particle Swarm Optimization (PSO). *Solar Energy* 86, 3137-3145, 2012.
- [5] C. Voyant and M. Muselli C. Paoli M. L. Nivet. Optimization of an artificial neural network dedicated to the multivariate forecasting of daily global radiation. *Energy*, 36, 348-59, 2011.
- [6] L. T. Wong and W. K. Chow. Solar radiation model. *Applied Energy*, 2001.
- [7] H. Q. Victor, J. Almorox, I. Mirzakhayot, and L. Saito. Empirical models for estimating daily global solar radiation in Yucatán Peninsula, Mexico. *Energy Conversion and Management*, 2016.
- [8] M. T. Y. Tadros, M. A. M. Mustafa, and M. Abdelwahab. Estimation of Global Horizontal Solar Radiation in Iraq. *International Journal of Emerging Technology and Advanced Engineering*, 2014.
- [9] V. Bahel, H. Bakhsh, and R. Srinivasan. A correlation for estimation of global solar radiation. *Energy*, Vol. 12, No. 2, 131-135., 1987.
- [10] K. Bakirci. Correlations for estimation of daily global solar radiation with hours of bright sun-shine in Turkey. *Energy*, 34(4), 485-501., 2009.
- [11] C. A. Gueymard. Clear-sky irradiance predictions for solar resource mapping and large-scale applications: Improved validation methodology and detailed performance analysis of 18 broadband radiative models. *Solar Energy* 86, 2145-2169, 2012.
- [12] A. Angstrom. Solar and terrestrial radiation. *Journal of the Royal Meteorological Society*, 50, 121-6, 1984.
- [13] J. Almorox and C. Hontoria. Global solar estimation using sunshine duration in Spain. *Energy Conversion and Management*, Volume 45, Issues 9-10, 1529-1535, 2004.
- [14] F. J. Newland. A study of solar radiation models for the coastal region of south China. *Solar Energy*, 31, 227-35., 1988.
- [15] S. Rehman and M. Mohandas. Artificial neural network estimation of global solar radiation using air temperature and relative humidity. *Energy Policy*, 63, 571-6, 2008.
- [16] M. A. Behrang, E. Assareh, A. Ghanbarzadeh, and A. R. Noghrehabadi. The potential of different Artificial Neural Network (ANN) techniques in daily global solar radiation modeling based on meteorological data. *Solar Energy*, 84, 1468-80, 2010.
- [17] M. A. Behrang, E. Assareh, A. R. Noghrehabadi, and A. Ghanbarzadeh. New sunshine-based models for predicting global solar radiation using PSO (particle swarm optimization) technique. *Energy*, Volume 36, Issue 5, 3036-3049, 2011.
- [18] Z. A. AlMostafa, A. H. Maghrabi, and S. M. AlShehri. Sunshine-based global radiation models: A review and case study. *Energy Conversion and Management*, 84, 209-216, 2014.
- [19] M. Vakilia, S.R. Sabbagh-Yazdib, K. Kalhorb, and S. Khosrojerdic. Using Artificial Neural Networks for Prediction of Global Solar Radiation in Tehran Considering Particulate Matter Air Pollution. *Energy Procedia* 74, 1205-1212, 2015.
- [20] J. D. Karalis, D. K. Pissimanis, and V. A. Notaridou. Estimation of Global, Direct and Diffuse Solar Radiation in Athens Under Clear Sky Conditions. *Archives For Meteorology, Geophysics, And Bioclimatology, Ser. B*, 31, 369-377, 1982.
- [21] D. Djafer and A. Irbah. Estimation of atmospheric turbidity over Ghardaia city. *Atmospheric Research* 128, 2013.
- [22] D. Djafer, A. Irbah, and M. Zaiani. Identification of clear days solar irradiance observations using a new method based on the wavelet transform. *Renewable Energy*, 101 347-355, 2017.
- [23] H. El Badaoui, A. Abdallaoui, and S. Chabaa. Using MLP neural networks for predicting global solar radiation. *The International Journal Of Engineering And Science*, Volume 2, Issue 12, 48-56, 2013.
- [24] M. Zaiani and D. Djafer. Atmospheric turbidity study using ground and orbit data. *International Journal of Latest Research in Science and Technology ISSN (Online): 2278-5299*, Volume 3, Issue 2, 12-18, 2014.
- [25] Ch. B. Perrin and Ch. Vauge. *Le gisement solaire. Evaluation de la ressource energetique . Technique et Documentation Lavoisier Paris*, 1982.
- [26] C. A. Gueymard. Direct solar transmittance and irradiance predictions with broadband models. Part I: detailed theoretical performance assessment. *Solar Energy* 74, 355-379, 2003.
- [27] Y. ELMghouchi, A. El Bouardi, Z. Choulli, and T. Ajzoul. Estimate of the Direct, Diffuse and Global Solar Radiations. *International Journal of Science and Research*, 2012.
- [28] K. Tahri. Simulation of Instant Energy Incident on Three Sensors: Application in the Cities of Algeria. *Journal of Electrical Engineering* 2, 143-151, 2014.
- [29] M. Capderou. *The Solar Atlas of Algeria, EPAU Tome I, II, III, Algiers, . 1986.*